SLAC-PUB-10817
astro-ph/0410007
October 2004

The relation between black hole mass and velocity dispersion at $z \sim 0.37$

Tommaso Treu[2,3,4], Matthew A. Malkan[2] & Roger D. Blandford[4,5]

ABSTRACT

The velocity dispersion of 7 Seyfert 1 galaxies at $z \sim 0.37$ is measured using high signal-to-noise Keck spectra. Black hole (BH) mass estimates are obtained via an empirically calibrated photoionization method. We derive the BH mass velocity dispersion relationship at $z \sim 0.37$. We find an offset with respect to the local relationship, in the sense of somewhat lower velocity dispersion at a fixed BH mass at $z \sim 0.37$ than today, significant at the 97% level. The offset corresponds to $\Delta \log \sigma = -0.16$ with rms scatter of 0.13 dex. If confirmed by larger samples and independent checks on systematic uncertainties and selection effects, this result would be consistent with spheroids evolving faster than BHs in the past 4 Gyrs and inconsistent with pure luminosity evolution.

Subject headings: galaxies: elliptical and lenticular, cD — galaxies: evolution — galaxies: formation

1. Introduction

The correlation of the mass of the central black hole (M_{BH}) with the spheroid velocity dispersion σ (Ferrarese & Merritt 2000; Gebhardt et al. 2000; hereafter BHS) links phenomena at widely different scales (from the pcs of the BH sphere of influence to the kpcs of the bulge). This demonstrates that galaxy formation and AGN activity are connected

[1]Based on data collected at Keck Observatory, operated by Caltech and the University of California.

[2]University of California at Los Angeles, CA 90095; ttreu@astro.ucla.edu, malkan@astro.ucla.edu

[3]Hubble Fellow

[4]California Institute of Technology. Pasadena, CA 91125

[5]Kavli Institute for Particle Astrophysics and Cosmology Stanford, CA; rdb@slac.stanford.edu

Work supported in part by the Department of Energy Contract DE-AC02-76SF00515

Stanford Linear Accelerator Center, Stanford University, Stanford, CA 94309
Submitted to Astrophys.J.Lett.

and several physical explanations have been proposed (e.g. Kauffmann & Haenhelt 2000; Monaco et al. 2000; Volonteri et al. 2003; Haiman, Ciotti & Ostriker 2004).

Interesting clues can be obtained from the cosmic evolution of empirical relations. Different scenarios – all reproducing the local BHS relation – predict different evolution. For example, in a pure luminosity evolution scenario of spheroids, σ would not change with time, while M_{BH} would increase as a result of accretion. A typical $10^7 M_\odot$ BH accreting at an average rate $0.01 M_\odot yr^{-1}$ (e.g., Sun & Malkan 1989), would double its mass in a Gyr. This would predict the M_{BH} at given σ to increase with time, possibly changing the slope of the BHS relation if the accretion rate is a function of M_{BH} (e.g. Small & Blandford 1992). In contrast, if spheroids grew faster than BH, σ at fixed M_{BH} could increase with time.

In this *Letter* we present the first results from an observational program aimed at measuring the cosmic evolution of the BHS relation. We measure the BHS relation for a sample of 7 Seyfert 1s at $z \sim 0.37$. This redshift is high enough to provide a time baseline over which we might expect evolution, yet low enough to be observationally practical.

2. Observations and analysis

2.1. Experiment Design and Sample Selection

The sphere of influence of supermassive BHs in galaxies at cosmological distances cannot be resolved even with the Hubble Space Telescope (HST). Therefore we target active galaxies, where M_{BH} can be obtained from the integrated properties of the broad emission-line region. In this paper, we will combine an empirically calibrated photo-ionization estimate of the size of the broad line region (hereafter ECPI; Wandel et al. 1999) with its kinematics measured from the rms width of Hβ, to deduce the central BH mass. To measure simultaneously the *stellar velocity dispersion* from absorption lines, requires nuclei of relatively low luminosity, so that the fraction of stellar light in the integrated spectrum is substantial. Seyfert 1s provide the right balance between the two components: absorption features typical of old stellar populations such as Mg5175 and Fe5270 are clearly visible in their high signal-to-noise integrated spectra. In order to minimize the uncertainties from sky subtraction and atmospheric absorption corrections, it is convenient to select specific redshift windows where the relevant emission and absorption lines fall in clean regions of the atmosphere. Accordingly, we selected the "clean window" $z \sim 0.37$, which corresponds to a look-back time of ~ 4 Gyrs, for $H_0 = 70\ \mathrm{km\,s^{-1}\,Mpc^{-1}}$, $\Omega_m = 0.3$, and $\Omega_\Lambda = 0.7$.

A first object (MS1558+453; hereafter S99; Stocke et al. 1991) was selected for a pilot study. When the Sloan Digital Sky Survey (SDSS) became available, a larger sample of

objects was selected according to the following criteria: $0.35 < z < 0.37$, Hβ equivalent width and rms width greater than 5 Å. These are sufficient to select only broad Hβ galaxies, but are loose enough that they should not introduce significant bias in M_{BH}. The relevant properties of the observed objects are listed in Table 1.

2.2. Observations and data reduction

High signal-to-noise (Table 1) spectra were obtained using the Low Resolution Imaging Spectrograph (Oke et al. 1995) at the Keck-I telescope on 2003 March 6 (S99) and 2003 Sep 3. Two exposures were obtained for each object, with total exposure times ranging between 1200s and 5280s. The 900/5500 grating with a 1.″5 slit provided a resolution of $\sigma_s = 55 \pm 5$ kms^{-1} around Mg5175 and Fe5270, as measured from sky lines and arc lamps. Internal flat fields were obtained after each object exposure, to correct the fringing pattern of the red CCD. A set of A0V stars from the Hipparcos catalog[1] to be $\lesssim 15$ degrees from each target was observed during the night as flux calibrators, and to measure the B-band atmospheric absorption. Spectrophotometric standards were observed during twilights. Internal tests, and comparison with SDSS spectra, show that this procedure corrects the B-band absorption to a level of a few parts in a thousand and relative flux calibration to a few percent. The data reduction was similar to that in Treu et al. (2001).

2.3. Bulge Kinematics

The stellar velocity dispersion of the bulge was obtained by comparing the spectral region corresponding to 5100-5300 Å with spectra of G-K giants as described in Treu et al. (2001). Briefly, the high resolution template stars were redshifted and smoothed to match the resolution of the instrumental setup, and convolved with gaussians in $\log\lambda$ space to reproduce the kinematic broadening. Then a low order polynomial representing the featureless continuum was added (using the pixel fitting code by van der Marel 1994). Small AGN emission features at vacuum wavelengths λ5160.33, λ5200.53, and λ5310.34 Å (van den Berk et al. 2001) were masked out during the fit. This procedure yields a velocity dispersion $\sigma_{\rm ap}$, a line strength γ, with uncertainties (Tab. 1). For each object, we performed a number of tests, varying the spectral range and the order of the polynomial used for continuum fitting. The results were found to be sensitive to these changes for 6/13 objects (the ones with shallower stellar absorption features and typically with stronger FeII AGN emission). The other

[1]URL http://www.gemini.edu/sciops/instruments/niri/NIRISpecStdSearch.html

7 objects (Fig. 2) yielded stable σ – changes much smaller than estimated errors – and were therefore considered reliable. We note that excluding the Mg region changes the velocity dispersion by less than the estimated errors (c.f. Barth, Ho & Sargent 2003). For simplicity and consistency with previous work we assume that the central velocity dispersion σ (i.e. within a circular aperture of radius 1/8 of the effective radius; Ferrarese & Merritt 2000) can be obtained as $\sigma = \mathcal{B}\sigma_{ap}$, with $\mathcal{B}$=1.1 $\pm$ 0.05. This assumes that the spheroids have an effective radius of 0.″5, are non rotating, their velocity dispersion profile is similar to that of early-type galaxies, and the disk contamination to the line profile is negligible.

2.4. Black hole mass determination

Black hole masses were determined using the empirical correlation between continuum luminosity and size of the broad line region (Wandel et al. 1999; Kaspi et al. 2000, Vestergaard 2002) and the width of the broad component of Hβ, summarized by: $M_{\rm BH} = 4.9 \cdot 10^7 M_\odot L_{5100}^{0.5} W_{3000}^2$ (Shields et al. 2003), where L_{5100} is the luminosity of the continuum at 5100 Å in units of 10^{44} erg s^{-1} and W_{3000} is the FWHM of the broad component Hβ in units of 3000 km s^{-1}(Note that adopting a different slope for L_{5100}, e.g. 0.66 in eq A5 in Vestergaard 2002, does not change our result because of the luminosity range spanned by our sample). This formula assumes that the regions emitting broad Hβ in all AGN are photoionized under the same conditions, by a UV continuum of the same shape. The bulk velocities of the emitting gas clouds are presumed to be dominated by gravity, an assumption for which there is currently moderate observational support (Peterson & Wandel 1999).

Absolute calibration of L_{5100} was obtained by normalizing the LRIS spectra to the model SDSS r' magnitude. Since SDSS photometry and LRIS spectra are obtained at different epochs, the flux normalization is uncertain by $\sim$ 20 % due to AGN variability (Webb & Malkan 2000). This introduces a random error component of $\sim$ 10% on $M_{\rm BH}$, which is negligible with respect to the intrinsic scatter of the ECPI method (a factor of $\sim$ 2.5, Vestergaard 2002). The L_{5100} flux was then corrected for Galactic extinction (Schlegel et al. 1998) and subtracted the portion produced by starlight, by comparing the measured line strength of the stellar features with an assumed standard intrinsic value of $\gamma = 0.75 \pm 0.25$ (van der Marel 1994). The starlight falling outside the slit, but included in the photometry, was estimated from the measured seeing (1.″0) and a $r^{1/4}$ profile for the host galaxy with effective radius 0.″5. The estimated fractions of AGN-to-total light $f_{\rm AGN}$ are listed in Tab. 1.

The high signal-to-noise and resolution of the spectra allowed us to determine the width of the broad component of Hβ using the following procedure (Fig. 2): *i)* the continuum was subtracted by fitting a straight line between the continua at 4700 Å and 5100 Å rest

frame. *ii)* The [O III] line at 5007Å was divided by 3 and blueshifted to remove the 4959Å line. *iii)* The [O III] line at 5007Å was blueshifted and rescaled to remove the narrow component of Hβ. The line ratio H$\beta_{\rm narrow}$ / [O III]λ5007 was allowed to range between 1/20 and the maximum value consistent with the absence of "dips" in the broad component (typically 1/10-1/7; e.g. Marziani et al. 2003). *iv)* The second moment of the residual broad Hβ component was computed for the minimum and maximum narrow Hβ. The average and semidifference of the two values were taken as best estimate and uncertainty of the broad Hβ rms. The rms was confirmed to be much more insensitive than the FWHM to continuum and narrow component subtraction (see also Peterson et al. 2004). *v)* The rms was transformed into FWHM assuming FWHM = 2.35 rms, consistent with the observed values (Peterson et al. 2004 report 2.03 ± 0.59. Their value would lower $M_{\rm BH}$ by ~ 34 %).

3. The Black Hole mass velocity dispersion relation at $z \sim 0.37$

The BHS relation is shown in Figure 3 and compared to the local relations (Merritt & Ferrarese 2001; Tremaine et al. 2002). Local AGN with reliable σ and $M_{\rm BH}$ from Ferrarese et al. (2001) are also shown for comparison. We stress that the plot should be interpreted with caution, since $M_{\rm BH}$ obtained with the ECPI method is uncertain by a factor of ~ 2.5, as opposed to the more precise estimates available for nearby objects. Furthermore, the distribution of errors is non-gaussian and estimates for individual objects may be significantly off, especially when based on single epoch measurements (Vestergaard 2002). Given the relatively large and non-gaussian uncertainties, selection effects could be playing an important, and hard to quantify, role. Selection effects enter in both quantities: σ of bulges smaller or close to the instrumental resolution (σ_s) cannot be reliably measured, while very large σ tend to dilute the absorption features and therefore are harder to measure at a given S/N. Our observational biases also limit the observable $M_{\rm BH}$ range. When we are signal-to-noise limited, and therefore flux limited, we might exclude objects with the smallest $M_{\rm BH}$ for a given σ. In contrast, by requiring detectable stellar features in the integrated spectrum we are excluding the brightest AGNs.

At face value, this result indicates that 4 Gyrs ago BHs lived in bulges with lower σ. The χ^2 of the 7 points with respect to the local relationship is 15.7, including errors on both quantities, i.e. the probability that they are drawn from the local relationship is 3%. Assuming that BH growth was negligible and adopting the local BHS slope, the average difference and scatter in the intercepts corresponds to -0.16 ± 0.13 dex in $\log \sigma$ at fixed $M_{\rm BH}$. Most of the offset and scatter is given by the galaxy with the smallest σ and largest fractional uncertainty (S05). Discarding that point, the offset and scatter are -0.12 ± 0.06

dex in $\log\sigma$. In terms of M_{BH}, the scatter around the relation is 0.6 dex, or 0.3 dex excluding S05. Since the estimated uncertainty on M_{BH} alone is ~ 0.4 dex, the intrinsic component of the scatter did not increase dramatically. Our result appears to be at variance with that by Shields et al. (2003), who combined ECPI M_{BH} with [O III] emission line width, to measure the BHS relation out to $z \sim 3$. Their result is consistent with no evolution, albeit with large scatter. More data are needed to understand the origin and significance of this discrepancy. Possible explanations include the different velocity dispersions adopted (stellar features vs [O III]) and the different range in M_{BH}. At this stage we refrain from quantifying the slope.

In order to confirm this tantalizing and perhaps surprising result, data for a larger and more complete sample will be needed, also to address two important systematic effects that could conspire to simulate the observed evolution. First, the local calibration of the ECPI method might not be appropriate for the distant universe. Reverberation mapping studies of distant galaxies could verify this. Second, the assumed relationship between σ and σ_{ap} should be checked independently. For example the contribution from a face-on cold disk could lower σ_{ap} requiring a higher value for $\mathcal{B}$, reducing the apparent evolution: $\mathcal{B}$=1.59 would be required to bring the $z \sim 0.37$ and $z \sim 0$ relationships in agreement. HST imaging is needed to determine the inclination and relative luminosity of the disk within the spectroscopic aperture, while higher signal-to-noise ratio and spatially resolved spectroscopy are needed to study departures from gaussianity of the line profile and rotational support.

4. Conclusions

We have measured the velocity dispersion of the hosts of distant active nuclei. In combination with M_{BH} estimates using the ECPI method, we have obtained a first estimate of the BHS relation at $z \sim 0.37$. Since M_{BH} cannot decrease, this measurement, taken at face value, suggests the σ of bulges of Sy1s increased by roughly 40% in the past 4 Gyrs. Having provided a first illustration of the method, it is now necessary to collect data for a large sample of objects spanning a larger range of M_{BH} and σ, and to test systematic uncertainties by obtaining independent measures of M_{BH} and spatially resolved information on the bulge and disk morphology and kinematics.

We thank A. Barth, G. Bertin, L.Ciotti, B.Hansen, L.V.E. Koopmans, S. Gallagher, and the referee for useful suggestions. The use of software developed by R. P. van der Marel is gratefully acknowledged. TT is supported by the NASA Hubble Fellowship grant HF-01167.01. This project relied upon the SDSS Database. The authors acknowledge the role of Mauna Kea within the Hawaiian community.

REFERENCES

Barth, A.J., Ho, L. C., Sargent, W.L.W. 2003, ApJ, 583, 134

Ferrarese, L. & Merritt, D. 2000, ApJ, 539, L9

Ferrarese, L., Pogge, R.W., Peterson, B.M., Merritt, D., Wandel, A. & Joseph, C.L. 2001, ApJ, 555, L79

Gebhardt, K. et al. 2000 ApJ, 539, L13

Haiman, Z., Ciotti, L., Ostriker, J.P. 2004, ApJ, 606, 763

Kaspi, S. et al. 2000 ApJ, 533, 631

Kauffmann, G. & Haenhelt, M. 2000, MNRAS, 311, 576

Marziani, P., Sulentic, J. W., Zamanov, R., Calvani, M., Dultzin-Hacyan, D., Bachev, R., Zwitter, T. 2003, ApJS, 145, 199

Merritt, D. & Ferrarese L. 2001, ApJ, 547, 140

Monaco, P. , Salucci, P. & Danese, L. 2000, MNRAS, 311, 279

Oke, B. et al. 1995, PASP, 107, 375

Peterson, B.M. & Wandel, A. 1999, ApJ, 521, L95

Peterson, B.M. et al. 2004, preprint, astro-ph/0407299

Schlegel, D.J., Finkbeiner, D.P., Davis, M. 1998, ApJ, 500, 525

Shields, G.A., Gebhardt, K., Salviander, S., Wills, B.J., Xie, B., Brotherton, M.S., Yuan, J. & Dietrich, M. 2003, ApJ, 583, 124

Small, T. & Blandford, R.D. 1992, MNRAS, 259, 725

Stocke, J. T., Morris, S.L., Goia, I.M., Maccacaro, T., Schild, R., Wolter, A., Fleming, T.A., Henry, J.P. 2001, ApJS, 76, 813

Sun & Malkan 1989, ApJ, 346, 58

Tremaine, S. et al. 2002, ApJ, 574, 740

Treu, T., Stiavelli, M., Møller, P., Casertano, S., Bertin, G., 2001, MNRAS, 326, 221

vanden Berk, D.E. et al. 2001, AJ, 122, 549

van der Marel, R. P. 1994, MNRAS, 270, 271

Vestergaard, M. 2002, ApJ, 571, 733

Volonteri, M. Haardt F., & Madau P. 2003, ApJ, 582, 559

Wandel, A., Peterson, B. & Malkan, M. 1999, ApJ, 526, 579

Webb, W. & Malkan, M.A. 2000, ApJ, 540, 652

Table 1. Summary of relevant measurements

ID	α_{2000}	δ_{2000}	S/N	z	$\sigma_{\rm ap}$	γ	f_{5100}	rms(Hβ)	$f_{\rm AGN}$	log ($M_{\rm BH}/M_\odot$)
S01	15:39:16.23	+03:23:22.06	36	0.3593	-	-	6.00±0.01	50.0±0.4	-	-
S02	16:11:11.67	+51:31:31.12	51	0.3543	-	-	5.24±0.01	41.8±1.1	-	-
S03	17:32:03.11	+61:17:51.95	65	0.3583	-	-	10.72±0.02	35.7±0.2	-	-
S04	21:02:11.51	−06:46:45.03	53	0.3577	140±17	0.34±0.13	7.77±0.01	50.2±1.1	0.44	8.18
S05	21:04:51.84	−07:12:09.45	54	0.3533	81±32	0.18±0.05	9.44±0.02	62.2±1.6	0.68	8.52
S06	21:20:34.18	−06:41:22.24	36	0.3686	123±31	0.24±0.09	8.85±0.02	45.6±0.6	0.58	8.21
S07	23:09:46.14	+00:00:48.91	65	0.3517	-	-	11.69±0.02	53.5±0.3	-	-
S08	23:59:53.44	−09:36:55.53	62	0.3583	139±23	0.21±0.08	8.62±0.01	27.2±0.5	0.63	7.77
S09	00:59:16.11	+15:38:16.08	46	0.3539	137±30	0.22±0.08	10.80±0.02	41.5±1.1	0.62	8.17
S10	01:01:12.07	−09:45:00.76	61	0.3509	-	-	14.46±0.02	42.1±0.8	-	-
S11	01:07:15.97	−08:34:29.40	55	0.3555	-	-	9.07±0.02	32.8±0.1	-	-
S12	02:13:40.60	+13:47:56.06	46	0.3579	161±36	0.26±0.07	13.70±0.03	72.0±0.7	0.55	8.66
S99	16:00:02.80	+41:30:27.00	49	0.3676	182±18	0.43±0.10	5.83±0.01	72.2±2.6	0.31	8.33

Note. — For each object we list coordinates, average signal-to-noise ratio per Å of the region used for the kinematic fit, redshift, velocity dispersion (in km s^{-1}), line strength, total flux at 5100 Å (rest frame; in 10^{-17} erg $s^{-1}cm^{-2}Å^{-1}$; corrected as described in Section 3; absolute flux calibration uncertainties are not included), rms width of the broad component of Hβ (in Å, observed frame), estimated fraction of AGN contribution to the flux at 5100Å, estimated $M_{\rm BH}$(the related uncertainty is ~ 0.4 dex).

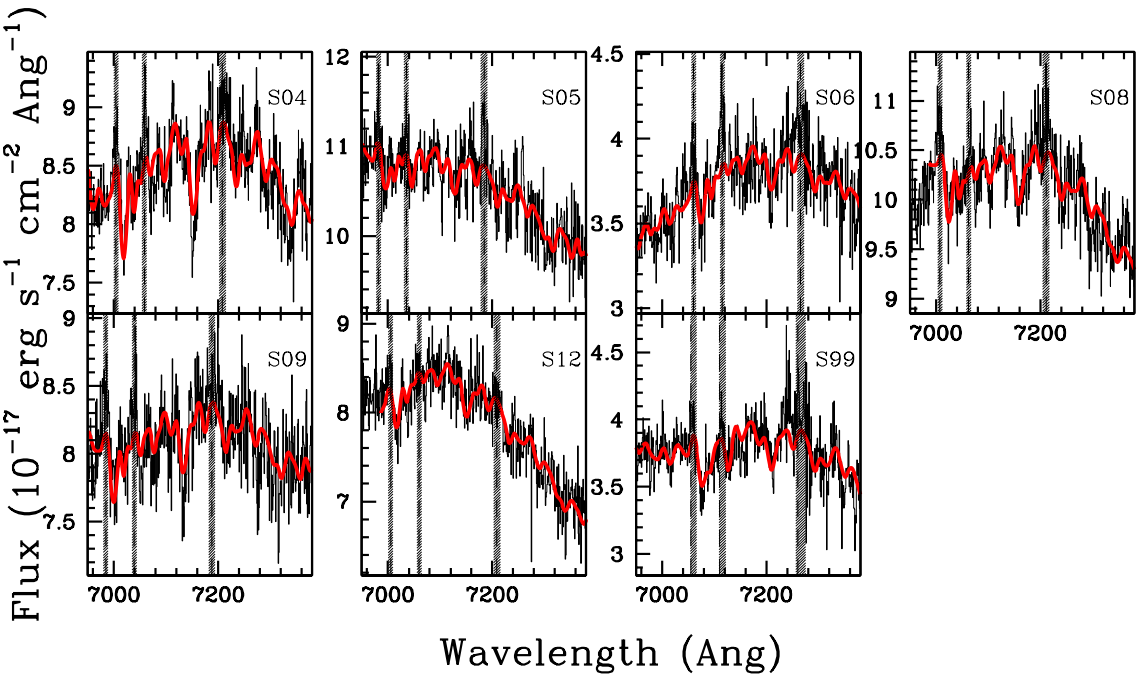

Fig. 1.— Portion of the spectra used to measure bulge kinematics. The black line is the data, the red lines is the best fit, shaded areas indicate regions masked out during the fit.

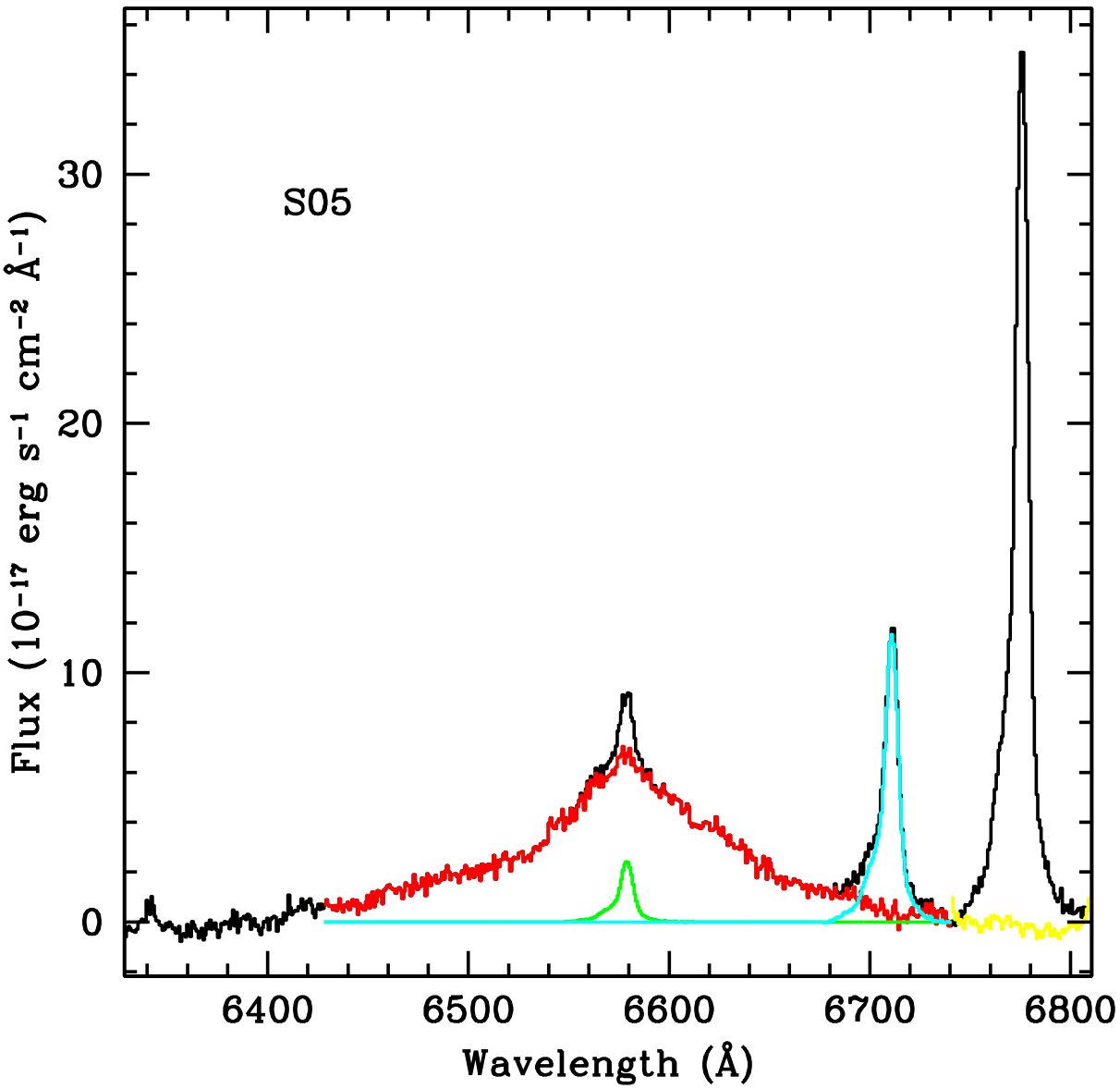

Fig. 2.— Example of Hβ width determination. The black line is the original spectrum after continuum subtraction. The cyan and green lines are the narrow components of [O III]λ4959 and Hβ respectively, obtained by rescaling and blueshifting [O III]λ5007. The red spectrum is the residual broad line used to compute the rms width. The yellow line underneath [O III]λ5007 is the reflection of the corresponding blue part of Hβ around its centroid.

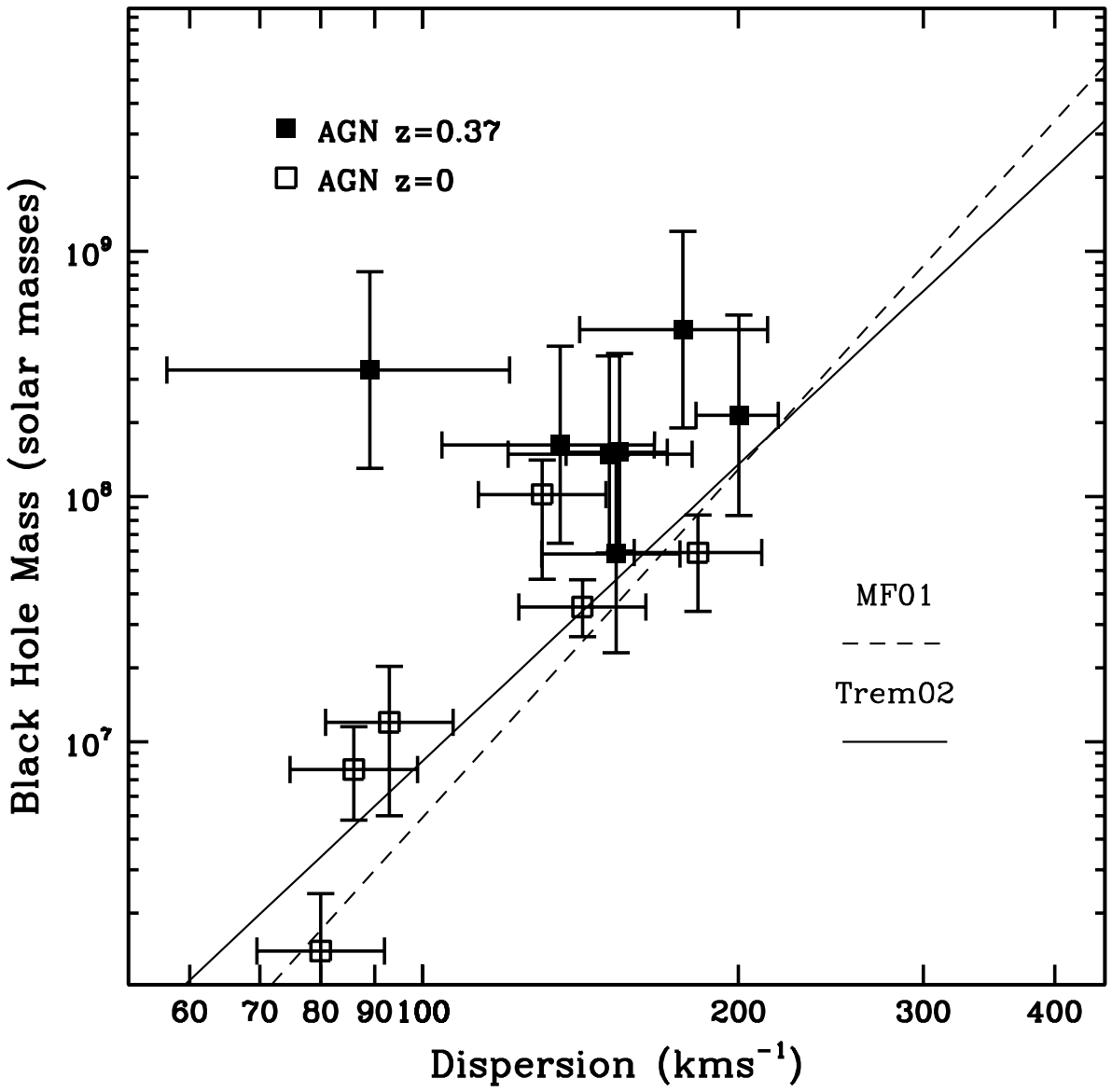

Fig. 3.— Black hole mass velocity dispersion relation at $z \sim 0.37$ (solid squares with error bars). The local relations by Merritt & Ferrarese (2001) and Tremaine et al. (2002) are also shown as solid and dashed lines. Since the latter adopts a slightly different definition of velocity dispersion, it is overplotted without corrections for comparison purposes only. Local AGN from Ferrarese et al. (2001) are shown as open points.